AD-A157 495 EXPERIMENTAL STUDY OF THE COMBUSTION OF GAS-AIR MIXTURES IN A CHANNEL AND..(U) FOREIGN TECHNOLOGY DIV WRIGHT-PATTERSON AFB OH V K BAYEV ET AL. 16 JUL 85 1/1

UNCLASSIFIED FTD-ID(RS)T-1323-84 F/G 21/2 NL

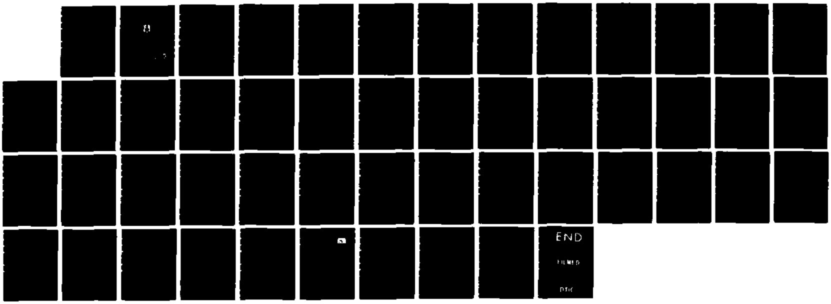

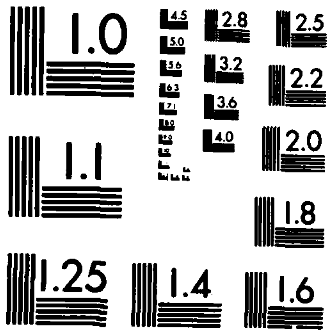

MICROCOPY RESOLUTION TEST CHART
NATIONAL BUREAU OF STANDARDS-1963-A

2

FTD-ID(RS)T-1323-84

FOREIGN TECHNOLOGY DIVISION

EXPERIMENTAL STUDY OF THE COMBUSTION OF GAS-AIR MIXTURES IN A CHANNEL AND THE DIFFUSION COMBUSTION IN A SLIPSTREAM AT HIGH VELOCITIES

by

V.K. Bayev, P.K. Tret'yakov, V.A. Yasakov

FTD-ID(RS)T-1323-84

UNEDITED MACHINE TRANSLATION

FTD-ID(RS)T-1323-84 16 July 1985

MICROFICHE NR: FTD-85-C-000526

EXPERIMENTAL STUDY OF THE COMBUSTION OF GAS-AIR MIXTURES IN A CHANNEL AND THE DIFFUSION COMBUSTION IN A SLIPSTREAM AT HIGH VELOCITIES

By: V.K. Bayev, P.K. Tret'yakov, V.A. Yasakov

English pages: 46

Source: Sovremennoye Sostoyaniye i Teoriya Sgoraniya Kondensirovannykh Sistem, Moscow, 1972, pp. 357-360; 386-391; 416-420; 421-425.

Country of origin: USSR
This document is a machine translation.
Requester: FTD/TQTA
Approved for public release; distribution unlimited.

Accession For	
NTIS GRA&I	X
DTIC TAB	☐
Unannounced	☐
Justification	
By	
Distribution/	
Availability Codes	
Dist	Avail and/or Special
A-1	

THIS TRANSLATION IS A RENDITION OF THE ORIGINAL FOREIGN TEXT WITHOUT ANY ANALYTICAL OR EDITORIAL COMMENT. STATEMENTS OR THEORIES ADVOCATED OR IMPLIED ARE THOSE OF THE SOURCE AND DO NOT NECESSARILY REFLECT THE POSITION OR OPINION OF THE FOREIGN TECHNOLOGY DIVISION.	PREPARED BY: TRANSLATION DIVISION FOREIGN TECHNOLOGY DIVISION WP-AFB, OHIO.

U. S. BOARD ON GEOGRAPHIC NAMES TRANSLITERATION SYSTEM

Block	Italic	Transliteration	Block	Italic	Transliteration
А а	*А а*	A, a	Р р	*Р р*	R, r
Б б	*Б б*	B, b	С с	*С с*	S, s
В в	*В в*	V, v	Т т	*Т т*	T, t
Г г	*Г г*	G, g	У у	*У у*	U, u
Д д	*Д д*	D, d	Ф ф	*Ф ф*	F, f
Е е	*Е е*	Ye, ye; E, e*	Х х	*Х х*	Kh, kh
Ж ж	*Ж ж*	Zh, zh	Ц ц	*Ц ц*	Ts, ts
З з	*З з*	Z, z	Ч ч	*Ч ч*	Ch, ch
И и	*И и*	I, i	Ш ш	*Ш ш*	Sh, sh
Й й	*Й й*	Y, y	Щ щ	*Щ щ*	Shch, shch
К к	*К к*	K, k	Ъ ъ	*Ъ ъ*	"
Л л	*Л л*	L, l	Ы ы	*Ы ы*	Y, y
М м	*М м*	M, m	Ь ь	*Ь ь*	'
Н н	*Н н*	N, n	Э э	*Э э*	E, e
О о	*О о*	O, o	Ю ю	*Ю ю*	Yu, yu
П п	*П п*	P, p	Я я	*Я я*	Ya, ya

*ye initially, after vowels, and after ъ, ь; e elsewhere.
When written as ё in Russian, transliterate as yё or ё.

RUSSIAN AND ENGLISH TRIGONOMETRIC FUNCTIONS

Russian	English	Russian	English	Russian	English
sin	sin	sh	sinh	arc sh	$\sinh^{-1}$
cos	cos	ch	cosh	arc ch	$\cosh^{-1}$
tg	tan	th	tanh	arc th	$\tanh^{-1}$
ctg	cot	cth	coth	arc cth	$\coth^{-1}$
sec	sec	sch	sech	arc sch	sech^{-1}
cosec	csc	csch	csch	arc csch	csch^{-1}

Russian	English
rot	curl
lg	log

GRAPHICS DISCLAIMER

All figures, graphics, tables, equations, etc. merged into this translation were extracted from the best quality copy available.

Page 357.

EXPERIMENTAL STUDY OF THE COMBUSTION OF GAS-AIR MIXTURES IN A CHANNEL AND THE DIFFUSION COMBUSTION IN A SLIPSTREAM AT HIGH VELOCITIES.

V. K. Bayev, P. K. Tret'yakov, V. A. Yasakov.

Novosibirsk.

In works [1-3] was shown possibility of criterial description of geometry of homogeneous and diffusion flames of disruption/separation, frequency flame front. The criterion of homochronicity $Ho = u\tau/d$, where u - rate, is basic criterion in this case; d - linear dimension; τ - characteristic combustion period, which determines physicochemical properties of mixture. The tables of characteristic times, comprised according to the experimental data, are given in [4, 5].

During diffusion combustion it is assumed that flame is spread in flow of homogeneous mixture of variable over section of composition. In this case as the characteristic combustion period its

minimum value (at identical temperatures of fuel/propellant and oxidizer for the approximately/exemplarily stoichiometric composition) is considered.

Intensity of turbulent exchange with jet-edge flow pattern can be characterized by length of nucleus of jet $\bar{X}_e$. During the combustion in the slipstream the intensity of exchange and, consequently, also $\bar{X}_e$ in the first approximation, depend on ratio $\rho_j u_j^2 / \rho_e u_e^2$ (ρ - density, j - fuel/propellant, e - oxidizer).

Basic purpose of this work was checking possibility of criterial description of processes of combustion in flows with high rates of flow.

1. Investigation of combustion of homogeneous mixture in channel with sudden expansion is carried out in combustion chamber with cross-section of 40×60 mm at discharge velocities at entrance to M=1.25 at temperature of stagnation at entrance ~300°K. The overall length of flame was determined according to the static pressure distribution and on the photometric measurement of straight/direct photography.

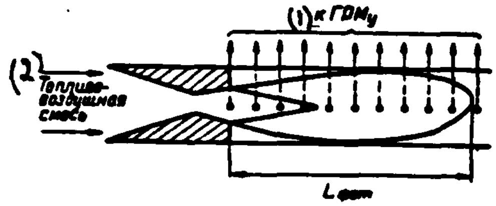

Fig. 1. Configuration of channel.

Keys: (1). to. (2). Fuel-air mixture.

Page 358.

The configuration of channel and the character of the distribution of pressure are represented in Fig. 1 and 2 respectively. Calculation by the curve of burnout according to the one-dimensional theory for this configuration of chamber/camera gives satisfactory results only at the relatively small distance from the end/lead of the flame. The results of determining the lengths of flames from the pressure and from the photometric measurement were compared with the calculation according to the formula for the flat duct

$$\bar{L} = (1-\varphi)\bar{X}_0\Theta^{1/2}\left(Ho^{1/2} + \frac{Ho}{\bar{x}_0}\right)^{2/3} + \varphi\bar{X}_0\Theta\left(Ho^{1/2} + \frac{Ho}{\bar{x}_0}\right), \qquad (1)$$

where φ - area ratio at entrance and output of channel;

Θ - ratio of the densities of fresh mixture and combustion

products;

$\bar{X}_{\bullet}$ - length of the nucleus of jet, which was being determined in this investigation by the visualization of flow with the isothermal blasting.

Comparison of calculation according to formula (1) with experimental data is represented in Fig. 3.

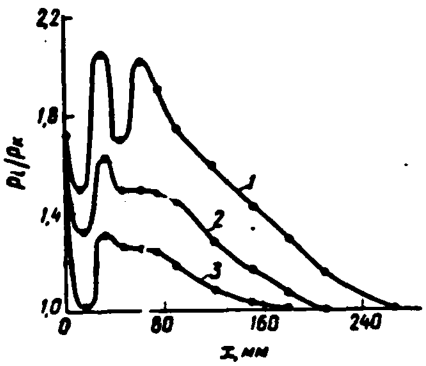

Fig. 2.

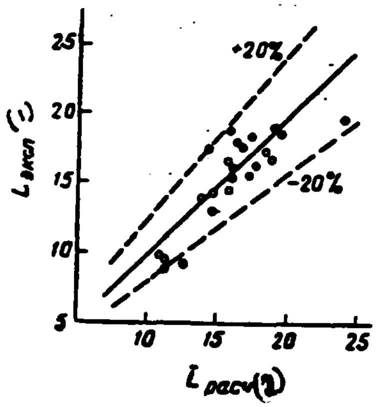

Fig. 3.

Fig. 2. Distribution of pressure along channel: 1 - M=0.81; α=1.10; 2 - M=0.98; α=1.32; 3 - M=1.19; α=1.80.

Fig. 3. Comparison of calculated and experimental lengths of flame: O - on photometric measurement; Δ - on pressure.

Keys: (1). L of exp. (2). $\bar{L}$ of calc.

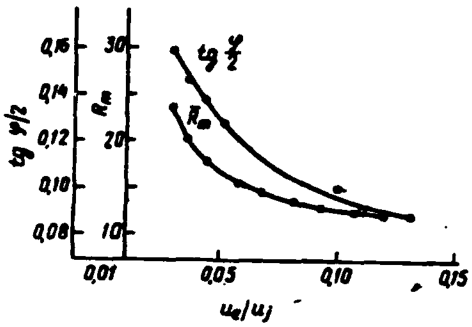

Fig. 4.

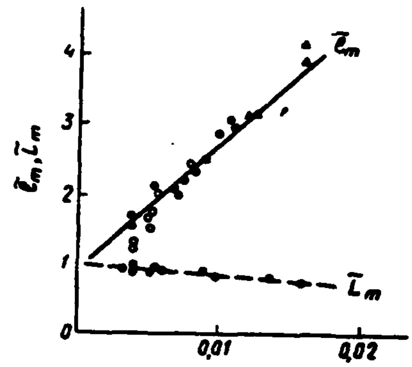

Fig. 5.

Fig. 4. Effect of cocurrent rate on expansion angle of jet and maximum radius of flame: ● - $d_j = 2{,}0$ mm; O - $d_j = 4{,}0$ mm.

Fig. 5. Change in length of breakaway and length of flame in unlimited cold slipstream: O - $d_j = 1{,}2$ mm; ● - $d_j = 2{,}0$ mm; ◇—$d_j = 3{,}0$ mm.

Page 359.

2. Combustion of hydrogen in cocurrent airflow they investigated during coaxial location of jet of hydrogen (diameters of nozzles $d_j = 1{,}2 - 4{,}0$ mm) and airstream ($d_e = 36$ mm). The first series of experiments is carried out with low speeds u_e (2-17 m/s) when $T_{0e} = T_{0j} = 300°K$. Fig. 4 gives the obtained dependences of the angle of expansion of the nonburning jet φ and the maximum relative radius of flame $\bar{R}_m$, while in Fig. 5 - a relative change in the length of

breakaway $\tilde{l}_m$ and relative change in the overall length of flame $\tilde{L}_m$ on the velocity ratio. Values $\tilde{l}_m = \bar{l}_m / \bar{l}_0$ and $\tilde{L}_m = \bar{L}_m / \bar{L}_0$ are the ratio of the length of breakaway and length of flame when $u_e/u_j \neq 0$ to the appropriate values when $u_e/u_j = 0$ with identical u_j. Moreover when $u_e/u_j = 0$, $\bar{l}_0 = \sqrt{\varrho/\varrho_e}$ *Ho* [3]. Value $\tilde{L}_m$ depends also on the relation of the diameters of nozzles. Analytical description in the investigated range can be represented as follows: $\tilde{L}_m = 1 - 0{,}8m\, d_e/d_j$. Flameout can be described by formula $u_j/u_e = d_j/d_e \cdot \frac{1}{m} - 1$.

At high rates of slipstream fire preheating of air for guaranteeing ignition conditions was realized. The parameters of modes/conditions and the results of criterial processing are represented in Fig. 6 in coordinates $lp^{1.7}/u_j - \rho_j u_j^2/\rho_e u_e^2$. The characteristic combustion period was determined by the extrapolation of dependence τ(T) with α=0.75 [4] in the high-temperature range. The dependence τ on the pressure is accepted by analogy with the dependence of the reaction time for hydrogen, given in work A. Ferri [6]. Values τ were taken at a temperature of stagnation of mixture. On the same graph/curve the data of A. Ferri [7], obtained during the electrical preheating of air on the installation of larger size/dimension, are given. One of the probable reasons for the stratification of curves for the different ones M and the disagreement with the data of A. Ferri is the presence of the narrow luminous zone from the nozzle edge to the zone of intense burnout (brightness), whose photometric

measurement is hindered/hampered. Other reasons can be the state of boundary layer to the surface of internal nozzle and the method of preheating air.

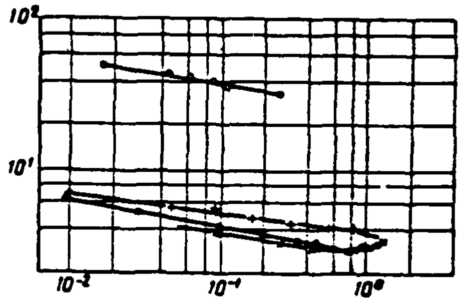

Fig. 6. The length of breakaway in the high-speed slipstream: * - Me=1.54 [7]; this work, ● - Me=1.58; X - Me=0.8; + - Me=0.6.

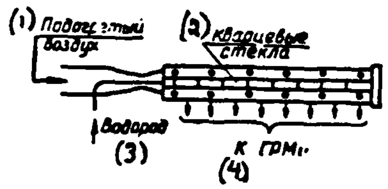

Fig. 7.

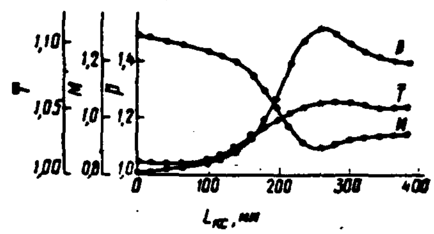

Fig. 8.

Fig. 7. Installation diagram.

Keys: (1). Heated air. (2). Quartz glass. (3). Hydrogen. (4). to.

Fig. 8. Change in flow parameters along channel.

Page 360.

Research of combustion of jet of hydrogen in channel of constant section was conducted with the same nozzle geometry. In the

experiments was measured the static pressure along the length of channel and they produced photographing of flame through the slot with a width of 10 mm, closed with quartz glass. The diagram of the installation is shown in Fig. 7, and the typical curves of a change in the pressure (measured) and the curves of a change in the temperature and Mach number along the channel, the calculated according to the distribution pressures taking into account of friction and heat exchange, they are given in Fig. 8. The results of the comparison of the calculated lengths of flame under these conditions (with respect to a change in the temperature) with the results of photometric measurement are represented in Fig. 9. The data of criterial processing of the length of breakaway and overall length of flame are cited in Fig. 10. The higher values of the lengths of breakaway in the channel in comparison with the open flames are explained, obviously, by the reason for that indicated it is above. It is interesting to note the approximately/exemplarily identical inclination/slope of curves for all data along the dimensionless length of breakaway when $\varrho_j u_j^2/\varrho_e u_e < 1$ (Fig. 6.10) and slope deviation of curve when $\varrho_j u_j^2/\varrho_e u_e^2 > 1$. Different character of effect $\varrho_j u_j^2/\varrho_e u_e^2$ attention is drawn to the length of breakaway and the overall length of flame.

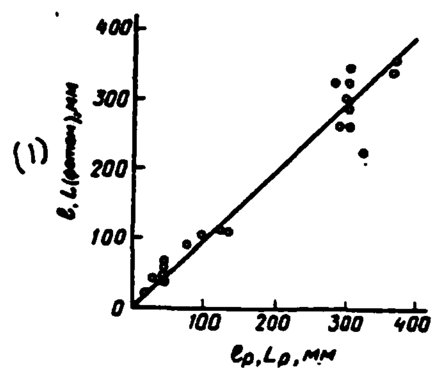

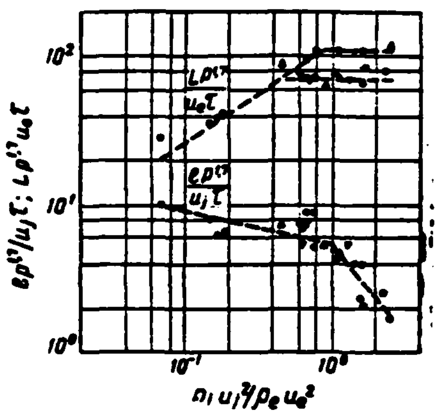

Fig. 9.

Fig. 10.

Fig. 9. Comparison of calculated and experimental lengths.

Keys: (1). (phot).

Fig. 10. Criterial generalization of length of breakaway and length of flame in channel of constant section: - Me=1.3; Δ - Me=0.68; -

Me=0.60; ◆ - Me=0.5-0.4.

REFERENCES.

1. В. К. Баев. Прикл. мех. и техн. физ., 1966, № 4 стр. 145—149.

2. В. К. Баев, П. К. Третьяков. Изв. СО АН СССР, сер. техн. наук, 1969, № 1, стр. 32—37.

3. В. К. Баев, В. А. Ясаков. Изв. СО АН СССР, сер. техн. наук, 1969, № 1, стр. 38—42.

4. В. К. Баев, П. К. Третьяков. Физ. гор. и взрыва, 1968, № 3, стр. 367—376.

5. В. И. Обмоин, П. К. Третьяков. Изв. СО АН СССР, сер. техн. наук, 1969, № 13, стр. 123—124.

6. A. Ferri. J. Roy. Aeronaut. Soc., 1964, 8, p. 575—595.

7. A. Ferri, P. A. Libby, V. Zakkay. Proc. of the Internat. Council. of the Aeronautical Sciences, Third Congress, Stockholm, 1962. Washington—London, 1964, p. 1089—1155.

Page 386.

IGNITION AND INTERRUPTION OF COMBUSTION IN THE STAGNATION ZONE DURING FLOW AROUND A FLAT STEP OR INDENTATION BY A SUPERSONIC FLOW OF COMBUSTIBLE MIXTURE.

V. L. Zimont, V. K. Ivanov, S. Kh. Oganesyan.

Moscow.

During flow around of step or indentation by nonreacting supersonic flow of combustible mixture in forming dead zone possible smooth burning, being characterized by specific critical parameters of flow, in which occurs blowout or its spontaneous emergence (ignition). In the case of the uniformity of the thermodynamic parameters in the stagnation zone with certain factors of ignition and interruption of combustion, together with the chemical kinetics, the mass exchange between the external flow and dead zone and the size/dimension of this zone (height/altitude of step or the depth of indentation h) are the factors of ignition and blowout. In this case (in contrast to the case of usual homogeneous chemical reactor) the

value of volume (V_g) of stagnation zone (during the flow around step) and the expenditure/consumption of mixture (G_g) flowing out from it depend on heat release.

Since in constant/invariable flow parameters - $G_g \sim h, V_g \sim h^2$ for step and $G_g \sim \mathrm{const}, V_g \sim h$ for indentation - usual reasonings about mutual location of curves, which present heat release during combustion and heat-escape due to mass exchange as functions of temperature in stagnation zone, show that both for step and for indentation there are always such heights/altitudes $h_I > h_{II}$, that when when $h > h_I$ occurs ignition in stagnation zone, and when $h < h_{II}$ - smooth burning in stagnation zone is impossible. Critical conditions for ignition and blowout for this thermal approach are

$$q_p = q_n, \quad \frac{dq_p}{dT} = \frac{dq_n}{dT},$$

where q_p and q_n - respectively heat release due to the chemical reaction and the heat loss per unit volume.

Page 387.

In the case of ignition, taking into account only heat losses, connected with mass exchange, and disregarding pre-explosion heating and change G_g and V_g (for step) connected with it, it is analogous with usual theory of thermal explosion [1], it is possible to obtain

relation between the parameters of stagnation zone, in which begins ignition. For example, in the case of the usual bimolecular reaction

$$q_p = Ae^{-E/RT} p^2 T^{-1.5} C_r C_0$$

critical retention time into the stagnation to zone, defined as

$$\tau_g = \frac{\rho_g V_g}{G_g},$$

is equal to

$$\tau_g = p_g T_g^{-2.5} \exp\left(B - \frac{E}{RT_g}\right),$$

where

$$B = \ln(2,718\, AC_r C_0 c_p^{-1});$$

c_p - specific heat;

ρ_g - gas density in the stagnation zone;

C_r and C_0 - concentration of fuel and oxidizer.

With chain/catenary mechanism ignition is connected with accumulation of active particles, whose concentration at initial moments of reaction taking into account mass exchange is described by relationship/ratio

$$\frac{dn}{dt} = \left(f - \frac{1}{\tau_g}\right) n,$$

where f - velocity coefficient in reaction of initiation of chains,

whence critical value of retention time in dead zone directly follows. For example, during the use as combustible hydrogen occurs the accumulation of atoms H. Utilizing a known kinetic relationship/ratio for this reaction [2], we will obtain expression for critical value τ_g through the parameters of gas in the stagnation zone

$$\tau_g = \frac{7.8 \cdot 10^{-12}}{p_g C_0} e^{\frac{18000}{RT_g}},$$

where C_0 - relative volumetric oxygen concentration;

p - pressure in the pressure in the bars.

Necessary for calculation parameters of separation zone were determined on the basis of diagram of flow, shown in Fig. 1. Flow in zone e was determined on the basis of relationships/ratios for the isentropic rarefaction wave, in this case a change in it in the thickness of initial (convergent from the wall) boundary layer was located on the basis of work [3].

In description of turbulent zone of mixing β model, proposed in work [4], was utilized. Under the assumption of normal density distribution of probabilities [4] the field of average/mean volume and mass concentrations in the layer of mixing is assigned in the form

$$C_e = 1 - C_g = \frac{1}{2}[1 + \Phi(\xi - \xi_c)]; \quad (1)$$

$$m_e = 1 - m_g = \frac{C_e}{C_e + \rho_g' \rho_e C_g}. \quad (2)$$

$$\Phi(z) = \frac{2}{\sqrt{2\pi}} \int_0^z e^{-t^2/2}\, dt$$

Here Λ - probability integral;

$\xi = y/\sigma$ - universal dimensionless coordinate.

Page 388.

In analogous form distribution of average speeds

$$\frac{u}{u_e} = \frac{1}{2}\left[1 + \Phi\left(\frac{\xi - \xi_c}{\sqrt{Pr_{эф}}}\right)\right]. \quad (3)$$

is described.

Effective value of number of Prandtl $Pr_{эф}$ was determined with enlistment of concept of "pole" (fictitious beginning of self-similar layer of mixing). In the absence of boundary layer ($\sigma_{x=0} = 0$) and with $x \to \infty$ was accepted value Pr=0.5. The significant dimension of the layer of mixing $\sigma(x)$ was calculated from the formula from work [5].

Coordinates of mid-position of profiles/airfoils (1) and (3) ξ_1, ξ_2 satisfy equations of conservation of mass flows and impulse/momentum/pulse in layer

$$\int_{\delta}^{\infty} d\xi - \frac{\delta^*}{x} = \int_{-\infty}^{+\infty} \frac{\bar{\rho}}{\rho_e} m_e \frac{u}{u_e} d\xi; \tag{4}$$

$$\int_{\delta}^{\infty} d\xi - \frac{\delta^* + \delta^{**}}{x} = \int_{-\infty}^{+\infty} \frac{\bar{\rho}}{\rho_e} \left(\frac{u}{u_e}\right)^2 d\xi, \tag{5}$$

where δ* and δ** - respectively displacement thickness and thickness of loss of pulse of boundary layer, which passed rarefaction wave with x=0.

Equation of conservation of flow of complete enthalpy is satisfied identically on the assumption that during braking of flow in layer due to dissipation is isolated supplementary heat

$$q(\xi) = c_p T_e \frac{k-1}{2} M_e^2 \frac{u}{u_e} \left(1 - \frac{u}{u_e}\right) \tag{6}$$

(M - Mach number). Analogously can be taken into consideration heat release in the layer of the mixing, which in this work is disregarded.

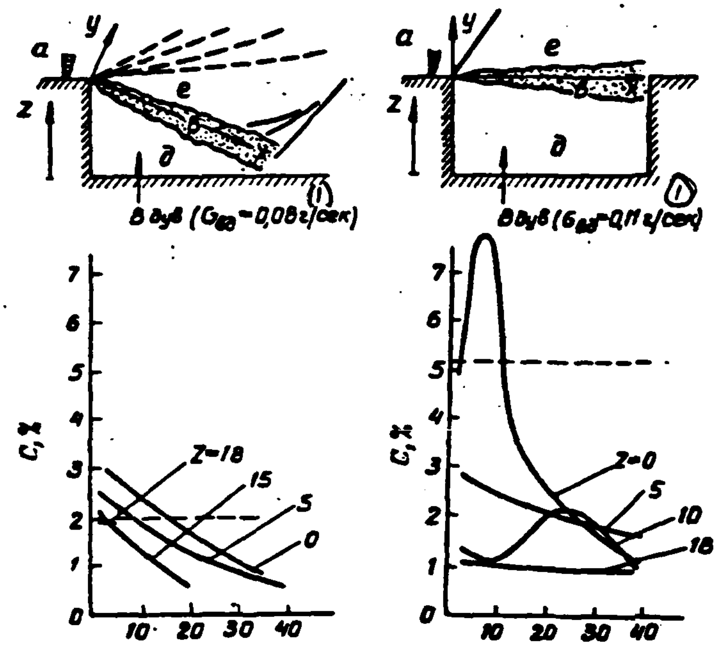

Fig. 1. Diagram of flow. Broken line - calculation, continuous - experiment.

Keys: (1). g/s.

Page 389.

Taking relation (6) into account, we have the distribution of average density

$$\frac{\bar{\rho}}{\rho_e} = \frac{C_e + \frac{\rho_g}{\rho_e} C_g}{1 + \frac{k-1}{2} M_e^2 \frac{u}{u_e}\left(1 - \frac{u}{u_e}\right)\left(C_e + \frac{\rho_g}{\rho_e} C_g\right)}.$$

Calulation of detached flow becomes locked with enlistment of conditions for conservation of mass and energy in stagnation zone during steady flow

$$\int_{\xi_0}^{\infty} \frac{\bar{\rho}}{\rho_e} m_g \frac{u}{u_e} d\xi = \int_{-\infty}^{\xi_0} \frac{\bar{\rho}}{\rho_e} m_e \frac{u}{u_e} d\xi + \frac{G_{bg}}{\rho_e u_e \delta^{*}}; \qquad (7)$$

$$\frac{T_g}{T_{0e}} \int_{\xi_0}^{\infty} \frac{\bar{\rho}}{\rho_e} m_g \frac{u}{u_e} d\xi = \int_{-\infty}^{\xi_0} \frac{\bar{\rho}}{\rho_e} m_e \frac{u}{u_e} d\xi + \frac{G_{bg} c_{pbg} T_{bg} + Q}{\rho_e u_e \delta^{*} c_p T_0}. \qquad (8)$$

where index bg designated parameters of blowing-in; Q - release of energy during combustion.

Coordinate of separating flow line ξ_0 was determined in accordance with Nash's criterion [6] for flow after step and directly from equation (7) for flow around indentation.

Flow of gas, which enters stagnation zone, and retention time were found by formulas

$$G_g = G_e = \rho_e u_e \delta^{*} \int_{-\infty}^{\xi_0} \frac{\bar{\rho}}{\rho_e} m_e \frac{u}{u_e} d\xi, \quad t = \frac{\rho_g V_g}{G_e + G_{bg}}.$$

Results of numerical calculations, carried out on computer(s) by S. Kh. Oganesyan by successive approximations, they showed good agreement with known experimental data on boundary layer effect, blowing-in, heat supply and combustion on parameters of gas in bottom region after step.

For checking validity of procedure of calculation of exchange accepted between dead zone and external flow were carried out

experiments on investigation of mass exchange after step and in indentation in the absence of combustion. In the experiments speed $M_a = 2{,}5$, Reynolds number $Re = \frac{u_a h}{\nu} \approx 4{,}3 \cdot 10^6$, the height/altitude of step and indentation 20, the length of indentation 40, the width of model is 175 mm, the length of plate from the spout of model to step and the indentation 130 mm, the thickness of initial boundary layer, according to calculation, $\delta/h=0.13$.

In stagnation zone through 19 openings/apertures with diameter of 1 mm, arranged/located evenly in series/row at a distance of 10 mm from side wall of step and indentation, was supplied small quantity of helium (0.1+0.2 g/s), which does not affect picture of flow and base pressure (in experiments $p_g/p_a = 0{,}4$, that are somewhat overstated in comparison with known experimental data [6]). The experimental profiles/airfoils of concentration of helium at the different heights/altitudes, obtained by chemical analysis, together with the results of calculations with the thickness of initial boundary layer indicated are given in Fig. 1. The designed concentrations correspond to theoretical retention times for the step and the indentation $1.3 \cdot 10^{-3}$ and $4.7 \cdot 10^{-3}$ s respectively.

Page 390.

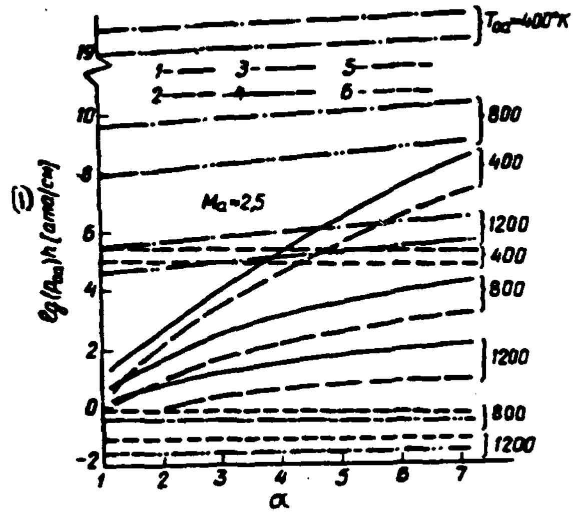

Fig. 2. The results of the calculations of the separation boundaries of combustion (the hydrocarbon fuel: 1 - step; 2 - indentation) and ignition (the hydrocarbon fuel: step; 3 - step; 4 - indentation and hydrogen: 5 - step; 6 - indentation) with constant M_a

Keys: (1). atm(abs.).

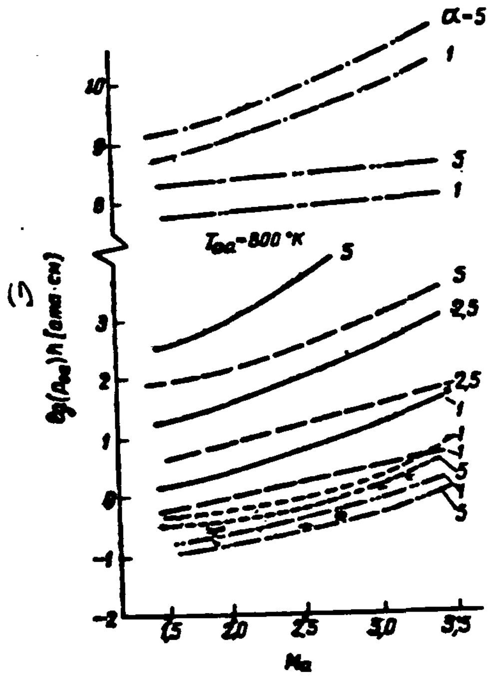

Fig. 3. The same as in Fig. 2, with fixed a.

Keys: (1). atm(abs.).

Page 391.

Fig. 2 and 3 for illustration give results of calculations of calculations of boundaries of ignition and blowout of hydrocarbon-air mixtures (for thermal mechanism) and ignitions of hydrogen-air mixtures (for chain/catenary mechanism) (α - coefficient of excess of oxidizer p_{0a} and M_a — are the total pressure and dimensionless rate of the inflowing mixture), obtained without taking into account initial boundary layer and with use of condition of Korst [7]. The heat release rate of

hydrocarbon-air mixture was determined on the basis of the total kinetic relationships/ratios, obtained for isooctane in work [8]; however, there is the foundation for hoping that the obtained estimations will be valid also for a broader class of hydrocarbon fuels, in particular, for the gasoline and kerosene [9].

In conclusion let us note that analogously can be determined critical boundaries with blowing-in of fuel directly into stagnation zone.

REFERENCES

1. Е. С. Щетинков. Физика горения газов. М., «Наука», 1965, стр. 176—183.
2. Л. А. Ловачев. II Всесоюзный симпозиум по горению и взрыву, авторефераты докладов. Черноголовка, 1969, стр. 86—92.
3. Р. К. Тагиров. Изв. АН СССР, Мех. жидк. и газов, 1966, № 2, стр. 145—149.
4. А. Г. Прудников, В. Н. Сагалович. В сб.: «Кинетика и аэродинамика процессов горения топлив» под ред. Б. В. Канторовича. М., «Наука», 1969, стр. 7—25.
5. R. S. Channapragada. AIAA-Journal, 1963, 1, No 9, p. 2188—2190.
6. I. F. Nash. An analysis of two-dimentional turbulent base flow, including the effect of the approaching boundary layer. ARC R. M., 1963, No 3344.
7. H. H. Korst. Osterr. Ingr-Arch., 1957, 1, No 3, p. 227—238.
8. I. Longwell, M. Weiss. Ind. Eng. Chem., 1955, 47, No 8, p. 1634—1643 (в сб.: «Вопросы ракетной техники», И.Л., 1956, № 6 (36), стр. 111—133).
9. В. Л. Зимонт, Ю. М. Трушин. Физ. гор. и взрыва, 1969, № 6, стр. 151—157.

Page 416.

COMBUSTION OF RICH KEROSINE-AIR MIXTURES IN TUNNEL TYPE CHAMBER.

V. I. Blinov, A. I. Lushpa, V. M. Khaylov, G. N. Khudyakov.

Moscow.

In recent years a series/row of works, dedicated to combustion of overenriched hydrocarbon-air mixtures, was published. On the flames of hydrocarbon gases were investigated questions of the formation of carbon black and heavy hydrocarbons [1-3], the integral emissivity of the generatrices of products [4], normal rates of combustion and limits of stabilization [5]. However, in the literature virtually they are absent by the excess air ratios $\alpha<1.0$ in industrial type chambers/cameras. Below are set forth the results of experimental combustion research of kerosine-air mixtures in the model of tunnel combustion chamber at a pressure 1.1 atm(abs.) and change α from 1.0 to 0.3. Was investigated the temperature effect of air (0-1000°C), length of the combustion chamber (0.5-2.0 m) and values α for the degree of approximation of composition and

thermodynamic parameters of combustion products to their values at the chemical equilibrium.

Experiments are carried out in experimental chamber/camera, schematically depicted in Fig. 1. Air, which enters the chamber/camera, was preheated in spiral type electrical preheater-resistance. In the initial conical section chambers/cameras 1 were established/installed: the swirl injector, directed against the airflow 2, flame holder in the form of hollow cone 3 and the igniting device/equipment in the form of spark plug 4. Basic part of the chamber/camera was the cylindrical multisection duct with an inside diameter of 100 mm 5. Sections were lined from within by electrocorundum, and therefore the losses through the wall did not exceed 5-8% of entire heat, which was being isolated in the chamber/camera. At the combustion chamber exit water-cooled graduated section 6 and exit cone 7 were established/installed. In the series/row of the sections of chamber/camera the temperature of gas with platinum-platinum-rhodium thermocouples 8 and the fields of total pressures by 9 were measured. The thermal condition of construction/design they judged by readings/indications of the thermocouples, welded to the chamber wall, and also immured at the specific depth into heatproof refractory lining 10. The sampling of combustion products for the gas analysis is produced with the aid of the intensely water-cooled separators of 11 two types - point, which

make it possible to determine a change in the concentrations over the section, and the averaging separators with 6 openings/apertures with a diameter of 2-3 mm, arranged/located along the equivalent areas.

Page 417.

Gas analysis of tests/samples is produced both with automatic gas analyzers of type GIP (on CO, CO_2, CH_4) and MGK (on O_2) and weight method (on CO, CO_2, CH_4, H_2O, O_2, H_2 and heavy hydrocarbons). In the figures given below the concentrations, measured by automatic gas analyzers, are designated by light points, and in a weight manner - dark/nonluminous. According to the data of weight gas analysis were determined the gas constant of combustion products (R), the value of relative heat release ($\overline{Q}_p$), which is the ratio of the isolated in the chamber/camera heat to maximally possible (with $\alpha=1.0$), and also the excess air ratio in the selected test/sample of gas.

For comparison of experimental data with theoretical ones according to equations of chemical equilibrium dependences of combustion temperature, composition of combustion products, gas constant and heat of reactions on excess air ratio and its temperature were designed with use of computer(s). Obtained data are plotted/applied in the figures by dotted lines.

Air flow rate in majority of experiments was 100 g/s, which corresponded to inlet velocity into combustion chamber 20-50 m/s. Pressure in all experiments was maintained/withstood at the level 1.1 atm(abs.). The duration of each experiment exceeded 15 min, which provided stationary thermal condition.

Experiments showed that with decrease α isolation/liberation of sooty particles in chamber/camera grows/rises. With $\alpha \leq 0.4$ in the series of experiments were observed the low-frequency oscillations/vibrations, which led to the partial decomposition of the heat-insulating coating of sections. As a result of the isolation/liberation in the chamber/camera of the sooty aerosol of rack/comb thermocouples and the probes were sufficiently rapidly covered/coated with carbonic/carbon outgrowth; therefore the results of measuring the temperature of gas in the chamber/camera during the analysis were not utilized. The results of measuring the concentrations at the end of the combustion chamber showed that the field of different components there is sufficiently flat/plane and the use of the averaging air intake was completely justified.

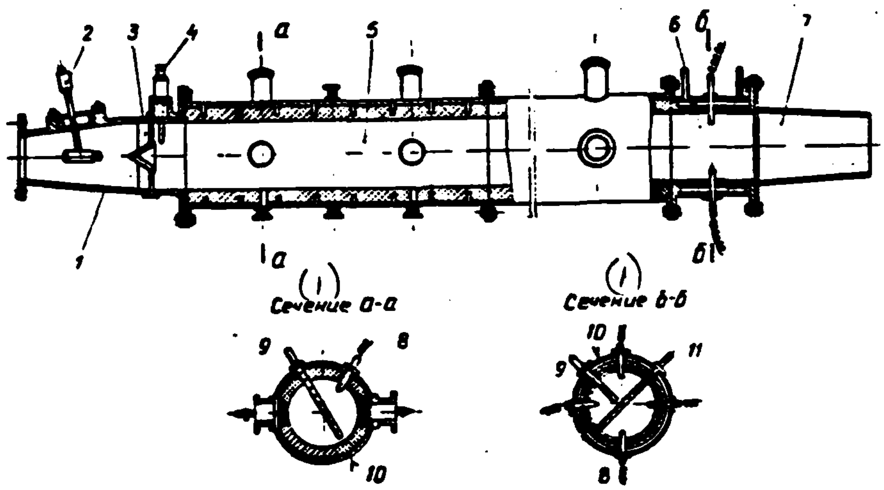

Fig. 1. Schematic diagram of the model of combustion chamber.

Key: (1). Section.

Page 418.

Fig. 2 shows dependence of concentrations CO and CO_2 at the end of combustion chamber on α at temperature of air 400 and 800°C. The results of measuring the concentrations H_2 in Fig. 2 are not plotted, the character of their change analogous to change CO.

Fig. 3 gives results of measuring concentrations CO, CO_2, H_2, O_2 with the aid of single-point air intake along axis/axle of combustion chamber. In all operating modes composition of combustion products along the length of chamber/camera differs from the theoretical,

moreover content CO and H_2 is less, and CO_2 are more than computed values. Percentage CO and H_2 with the displacement/movement toward the end of the chamber/camera increases, and CO_2 decreases. In the initial sections of chamber/camera free oxygen is present. At the length of chamber/camera of approximately two meters free oxygen virtually is absent, and the content of methane is negligibly small.

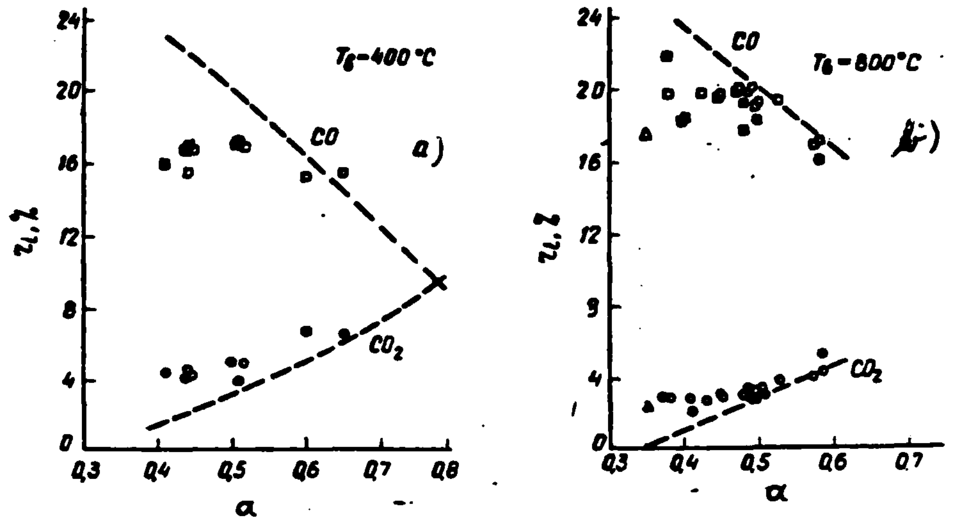

Fig. 2. Effect a the temperature of air ($T_в$) in volume fractions CO and CO_2 at the end of the combustion chamber. The dehydrated combustion products, the length of chamber/camera is 2.25 m.

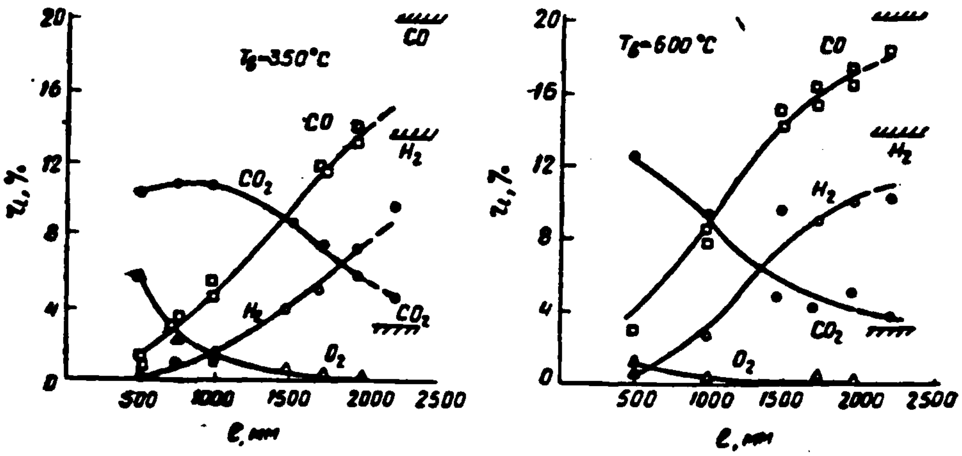

Fig. 3. Change along axis/axle of chamber/camera of volume fractions CO, CO_2, H_2 and O_2 α=0.5. Lines with the shading - computed values of concentrations.

Page 419.

As can be seen from example, given in Fig. 4, values of gas constant in the beginning of chamber/camera are less, and relative heat of reactions in selected test/sample of gas of higher than theoretical values approach them with increase in length of chamber/camera. Calculations showed that a change α in the gas part of the test/sample is analogous with change $\bar{Q}_p$. The less a and the lower the temperature of air, the flatter the curves of a change in the parameters of combustion products along the length of chamber/camera become and the stronger the deviation of their values from the theoretical ones proves to be. At a distance of 0.7-1.0 m from the stabilizer the fields of concentrations are strongly nonuniform, but at the length chambers/cameras 1.5-2.0 m are equalized virtually completely.

Analysis of obtained experimental data made it possible to compose qualitative picture of process of combustion under conditions in question. Apparently, in the beginning of chamber/camera, as a result of the nonuniform distribution of kerosene over the section, mixture burns with the values α, substantially those higher, than designed according to the flow rates of air and fuel/propellant. With

this CO_2 and H_2O it is isolated more, and CO and H_2 are less than the theoretical quantity, which corresponds to averaged-mass α. The increased heat release in the initial section contributes to the accelerated thermal decomposition of fuel/propellant, which is accompanied by the isolation/liberation of carbon, which plays large role subsequently the course of process. In the region, where there is no free oxygen already virtually, solid carbon (carbon black) is oxidized as a result of restoration/reduction CO_2 and H_2O. With the course of these reactions the temperature descends, which retards process. When the solid phase of reaction is present, they flow/occur/last considerably slower than in the homogeneous gas system.

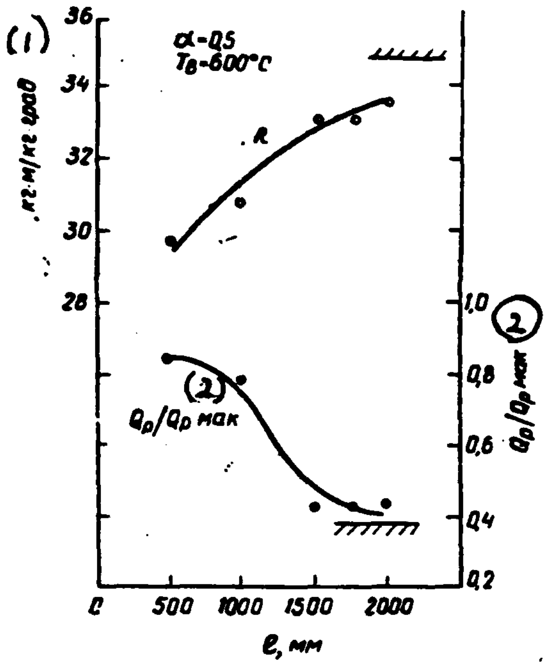

Fig. 4. Change along the axis/axle of the chamber/camera of the gas constant of the products of combustion R and relative heat release $\bar{Q}_p$. Lines with the shading - computed values.

Key: (1). kg·m/kg·deg. (2). max.

Page 420.

Because of this the process of the establishment of equilibrium composition in our case it is limited by a heterogeneous oxidation of solid carbon. The higher the temperature of air, the higher the temperature of combustion products and the more rapidly the state of

equilibrium sets in. An increase of α also increases the perfection of process, since in this case decreases the quantity of the carbon black, which was isolated in the primary zone and the temperature of combustion products simultaneously grows/rises. It is possible that the formation of solid carbon under the conditions in question can be somewhat suppressed, utilizing the metal-containing inhibitors recommended in work [1]. This question requires special investigation.

REFERENCES

1. G. Spengler, G. Haupt. Erdöl und Kohle, 1969, 22, No 11, S. 679.
2. J. J. Macfarlane. Combustion and Flame, 1970, 14, No 1, p. 67.
3. R. Lisbet, J. Combourien, A. Barassin, G. Morel. C. r. Acad. Sci., 1968, C206, No 9, p. 593.
4. А. Е. Еринов и др. Газовая промышленность, 1970, № 9, стр. 28.
5. Н. В. Лавров, С. Ф. Евланов. Газовая промышленность, 1970, № 6, стр. 42.

Page 421.

MECHANISM OF THE PROCESS OF COMBUSTION AFTER THE FRONT DEVICES AND IN THE ZONE OF THE INFLOW OF THE JETS OF SECONDARY AIR IN THE CHAMBERS OF GAS-TURBINE ENGINE.

G. M. Gorbunov, I. L. Khristoforov.

Moscow.

Experimental combustion research in nose section of flame tubes and on jets of secondary air in models of combustion chambers of aircraft gas-turbine engines (GTD) is carried out on installation (Fig. 1), in which were used typical front devices/equipment, undertaken from series chambers/cameras and which are characterized by method of introduction/input of primary air into flame tube.

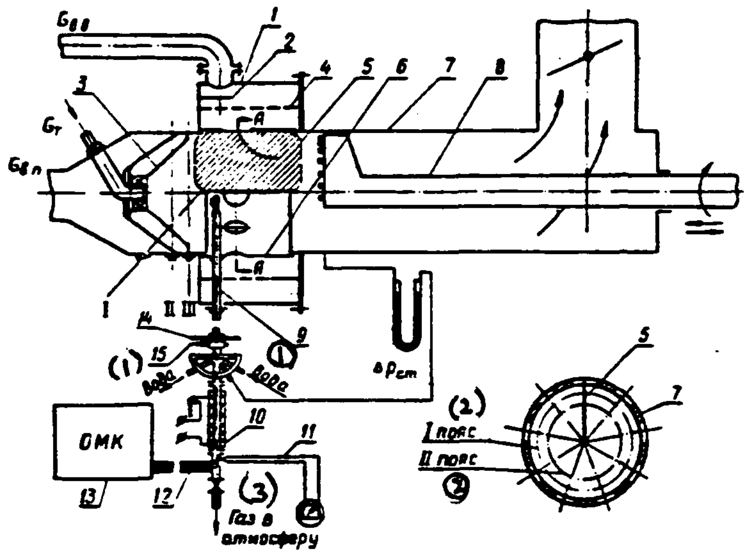

Fig. 1. The schematic of the test section of the installation: 1 - duct of the supply of secondary air; 2 - sector deflectors; 3 - cap/knob of combustion chamber; 4 - leveling grid; 5 - fixing plate; 6 - ring-inset; 7 - flame tube; 8 - rod with thermocouples or tubes of gas selection; 9 - separator of mixture; 10 - tubular electric furnace; 11 - thermocouple; 12 - heat-insulated tube; 13 - instrument OMK; 14 - limb/dial; 15 - arrow/pointer.

Key: (1). Water. (2). flange. (3). Gas in the atmosphere.

Page 422.

For propellant atomization (kerosene T-1) swirl injectors of corresponding production engines were utilized. In all experiments

maintained constant the following parameters: $p_k = 2.5$ atm(abs.); $T_k = 350°K$ and V=0.6 m³/s ($G_a = 1.5$ kg/s). Furthermore, separate air supply made it possible to maintain with constant relation of the flow rates between the primary and secondary air. The excess air ratio by primary air (G_{an}), introduced through the front device/equipment, always comprised $\alpha_n = 0.4$ (typical value for many chambers/cameras of production engines). The secondary air, supplied through one flange of openings/apertures in ring-inset, in all experiments led the total value of the excess air ratio to $\alpha_\Sigma = 1.5$. In given experiments the secondary air was introduced nine times by the openings/apertures with a diameter of 40 mm. The mean-expenditure air speed in the openings/apertures was w_a=30 m/s, which is also typical for the first flange of the openings/apertures of chamber/camera GTD. Further along the length of flame tube air was not supplied. In the technical furnaces during the combustion of different fuels/propellants in air depending on the method of organizing the process of combustion different diagrams of burnout can be accomplished/realized. Extreme typical will be the cases: the burnout of homogeneous mixture with the premixing of fuel/propellant with air and diffusion combustion during the separate feed of fuel/propellant and air to combustion zone. Can be observed, as it is known [1, 2], and the mixed, intermediate cases. What diagram of burnout will be accomplished/realized in this or another concrete/specific/actual combustion system, it is not always possible previously to predict.

This can be set from experiment, if the character of a change in the plots of the fields of temperatures T and local concentrations of fuel/propellant $u_{м}$ in the zone of burnout is known. With the burnout of the previously agitated mixture, ignited from the slipstream of hot gases, the change T and $u_{м}$ across the combustion zone occurs in the opposite directions, i.e., the decrease of concentration corresponds to an increase in the temperature. During the diffusion process of the burnout of propellant vapors, agitated with the hot gases, in the cocurrent airflow of value T and $u_{м}$ are changed to one side, i.e., an increase in the concentration (Fig. 2) corresponds to an increase in the temperature. In the chamber/camera with the front device/equipment, formed by the swirl vane and sleeve, in several directions (section I, II, III) they investigated the fields of temperatures, velocities and local concentrations of fuel/propellant. The results of these measurements (in section II) are given in Fig. 3 (in sections the I and III graphs/curves are not plotted/applied not in order not to encumber drawing).

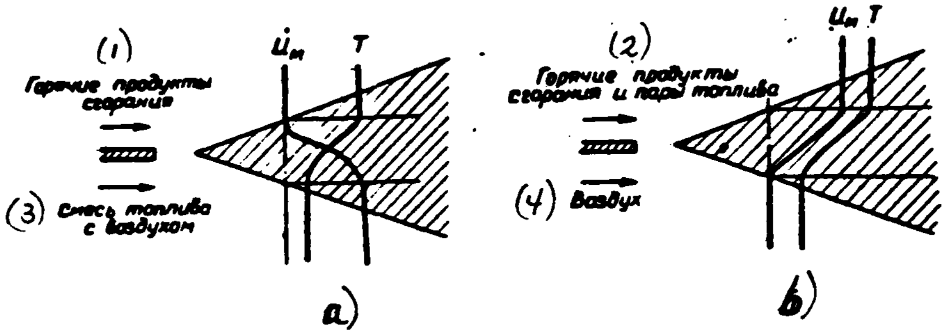

Fig. 2. Character of change T and $u_м$ in the zone of the burnout: a) with the preliminarily agitated mixture; b) with the diffusion combustion.

Key: (1). Hot combustion products. (2). Hot combustion products and propellant vapors. (3). Mixture of fuel/propellant with air. (4). Air.

Page 423.

Basic part of the fuel/propellant moves along the walls of sleeve and flame tube. Fuel evaporation and formation of fresh mixture here occurs. Into the combustion zone, shown by shading, enters the mixture, overenriched by fuel/propellant. Therefore after combustion zone is a residual propellant. Burnout, as graphs of change T have shown and $u_м$, occurs according to diagram I:

Гетерогенная (1) топливно-воздушная (4) смесь → Зона горения (3) → Продукты сгорания (2) (избыточное топливо) (5)

Key: (1). Heterogeneous. (2). Combustion products. (3). Combustion zone. (4). fuel-air mixture. (5). (surplus fuel/propellant).

In the zone of the inflow of the jets of secondary air, where, as is known, 80-85% of entire introduced into the chamber/camera fuel/propellant [3-5] burn; also were conducted the numerous measurements T and u_* both in the plane, which coincides with the axis/axle of jet, and on the cylindrical surfaces with different radii. Furthermore, was utilized the method of the "fixing plate" for studying the picture of combustion around jet [6]. In the plane, which coincides with the axis/axle of jet, the plate made of the stainless steel was established/installed and they started chamber/camera on 3-5 min. The temper color and deposit of carbon black they gave supplementary information about the depth of the penetration of jet, the location of the zones of burnout (Fig. 4).

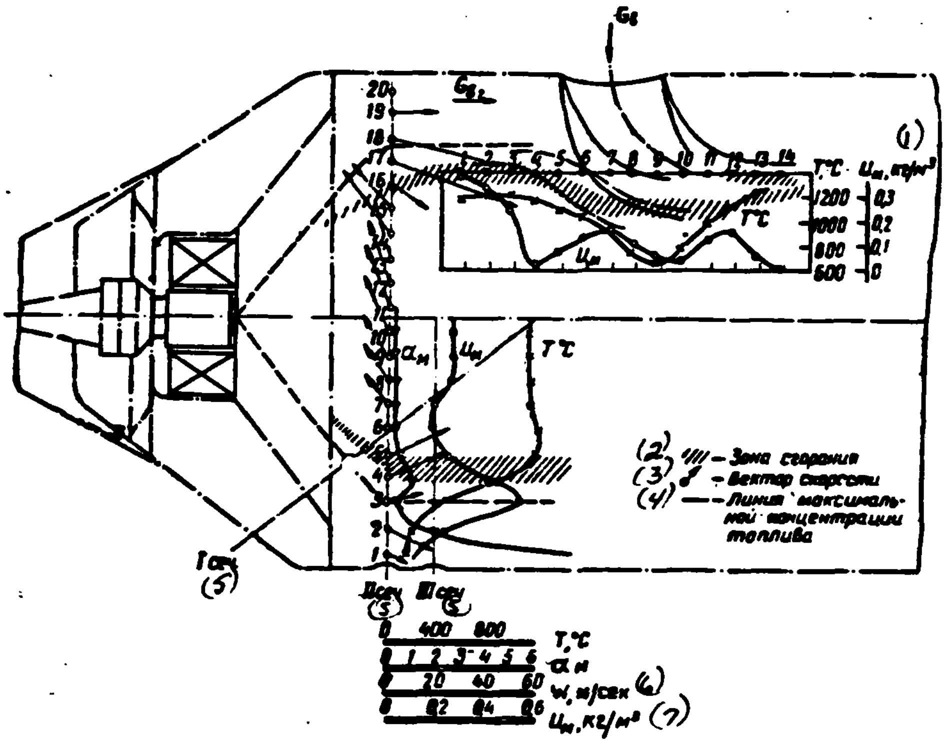

Fig. 3. The results of measurements in the chamber/camera with the front device/equipment of engine RD-500: $\alpha_м$ - fuel/propellant concentration; t - temperature of gases in °C; $\alpha_м$ - the local importance of the excess air ratios.

Key: (1). kg/m³. (2). Combustion zone. (3). Velocity vector. (4). Line of maximum concentration of fuel/propellant. (5). section. (6). m/s. (7). kg/m³.

Fig. 4. Photograph of "fixing plate".

Page 424.

The analysis of isotherms on the cylindrical surfaces, which intersect jet, leads to the conclusion that burnout occurs around the jet as this was earlier shown in the experiences of E. L. Solokhin [4]. To combustion zone on the jet (see Fig. 3) enters fresh mixture. An increase in the temperature in the combustion zone is accompanied by the decrease of fuel/propellant concentration, i.e., the mechanism of burnout here the same as in the cap/knob of chamber/camera.

Fig. 5 gives results of measurements in chamber/camera with round head, where primary air through system of punch-outs is supplied with thin film along internal walls of hemisphere. Here in the zone of burnout in the nose section of the chamber/camera and in the zone of burnout around the jet the increase of fuel/propellant concentration accompanies an increase in the temperature, i.e., is accomplished/realized the diffusion process of burnout, which takes place according to diagram II:

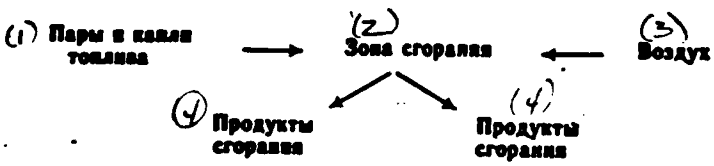

Key: (1). (1). Vapors and drop of fuel/propellant. (2). Combustion

zone. (3). Air. (4). Combustion products.

Thus, obtained results and their analysis made it possible to establish that if after front device/equipment of flame tube is realized process of burnout according to diagram I or diagram II, then respectively the same diagram I or II is realized with burnout around jets of first flange of openings/apertures for secondary air injection.

Does arise natural question, which of processes is preferable?

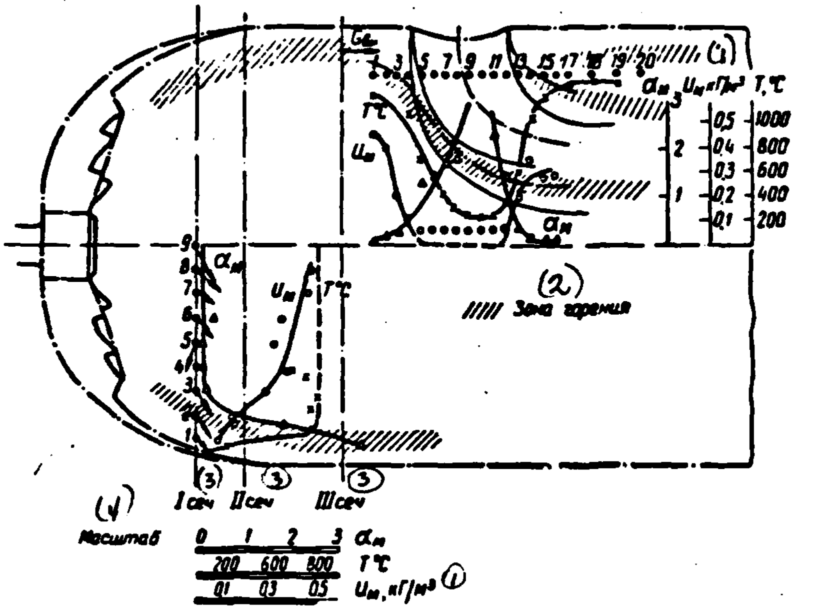

Fig. 5. Results of measurements in the chamber/camera with the hemispherical engine head VD-7. u - fuel/propellant concentration; t - temperature of gases in °C. α - local importance of the excess air ratios.

Key: (1). kg/m³. (2). Combustion zone. (3). section. (4). Scale.

Page 425.

On investigations of authors [6] value of combustion efficiency and length of chamber/camera, on which is reached one or the other combustion efficiency, were found to be dependent on parameters of

openings/apertures of secondary air (relative pitch of holes with specific depth of feed), i.e., from intensity of mixing in zone of supply of secondary air, but not from diagram of process of burnout.

Radiation from flame, as it is known [2], large during diffusion process of burnout. Therefore in the chamber/camera with the diffusion process to more complicatedly ensure the reliable cooling of the walls of flame tube, but in it it is possible to obtain best stalling characteristics.

At present selection of chambers/cameras with one or the other working process depends, probably, not so much by their specific special features/peculiarities, as by traditions and by available work experience.

REFERENCES

1. Е. С. Щетинков. Физика горения газов. М., «Наука», 1963.
2. Г. Ф. Кнорре, К. М. Арефьев, А. Г. Блох, Е. А. Нахапетян, И. И. Палеев. Теория топочных процессов. М., «Энергия», 1966.
3. Б. В. Раушенбах, С. А. Белый, И. В. Беспалов, В. Я. Бородачев, М. С. Волынский, А. Г. Прудников. Физические основы рабочего процесса в камерах сгорания воздушно-реактивных двигателей. М., «Машиностроение», 1964.
4. Исследование рабочего процесса в камерах сгорания газотурбинных двигателей. Сб. под ред. Г. М. Горбунова. М., «Машиностроение», 1964.
5. Г. М. Горбунов, И. Л. Христофоров. Механизм выгорания топлива и тепловыделение в зоне втекания струй вторичного воздуха в камере ГТД с различными фронтовыми устройствами. Изв. ВУЗов, «Авиационная техника», № 1, 1970, стр. 88—96.
6. Г. М. Горбунов, В. Л. Трусов, И. Л. Христофоров. О механизме выгорания топлива в зоне втекания струй вторичного воздуха в камере сгорания ГТД. Изв. ВУЗов, «Авиационная техника», № 4, 1967, стр. 100—108.

END

FILMED

9-85

DTIC